Theoretical approaches to low energy $\bar{K}$N interactions

Aleš Cieplý

Nuclear Physics Institute, Řež/Prague, Czechia

NESON2016, Krakow, June 6, 2016

Outline:

1. Introduction, experimental data
2. Chirally motivated $\bar{K}N$ approaches
3. Model predictions
4. Dynamically generated poles
5. Summary

A. C., M. Mai, U.-G. Meißner, J. Smejkal - Nucl. Phys. A (in print), arXiv:1603.02531[hep-ph]

Introduction

$\bar{K}N$ interactions

strongly interacting multichannel system with an s-wave resonance near threshold

involved channels	$\pi\Lambda$	$\pi\Sigma$	$\bar{K}N$	$\eta\Lambda$	$\eta\Sigma$	$K\Xi$
thresholds (MeV)	1250	1330	1435	1660	1740	1810

modern theoretical treatment based on an effective chiral Lagrangian
perturbation series do not converge in the vinicity of resonances!
$\Lambda(1405)$ (s-wave) and $\Sigma(1385)$ (p-wave) in between the $\pi\Sigma$ and $\bar{K}N$ thresholds

Solution: construct effective potentials, then use Lippman-Schwinger equation to sum the major part of the perturbation series

$$T = V + V\ G\ T$$

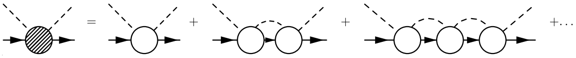

most approaches - only the s-wave considered

Experimental data

- K^-p low energy cross sections
  old buble chamber data on $K^-p \to K^-p,\ \bar{K}^0 n,\ \pi^0\Sigma^0,\ \pi^+\Sigma^-,\ \pi^-\Sigma^+$ at low energies
- K^-p threshold branching ratios

$$\gamma = \frac{\sigma(K^-p \to \pi^+\Sigma^-)}{\sigma(K^-p \to \pi^-\Sigma^+)} = 2.36 \pm 0.04$$

$$R_c = \frac{\sigma(K^-p \to \text{charged particles})}{\sigma(K^-p \to \text{all})} = 0.664 \pm 0.011$$

$$R_n = \frac{\sigma(K^-p \to \pi^0\Lambda)}{\sigma(K^-p \to \text{all neutral states})} = 0.189 \pm 0.015$$

- kaonic hydrogen data (SIDDHARTA, 2011)
  energy shift $\Delta E_N(1s) = 283 \pm 36(stat.) \pm 6(syst.)$ eV
  decay width $\Gamma(1s) = 541 \pm 89(stat.) \pm 22(syst.)$ eV

Experimental data

$\pi\Sigma$ mass distribution: comparison with results taken from three "compatible" experiments: Thomas (1973), Hemingway (1984), ANKE (2008).
HADES (2013) would fit in nicely too.

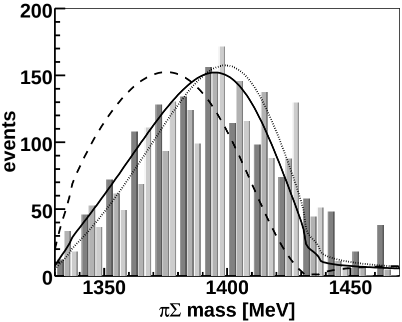

A. C., J. Smejkal - Nucl. Phys. A 881 (2012) 115

$$dN_{\pi\Sigma}/dM \sim \left| T_{\pi\Sigma,\pi\Sigma}(I=0) + r_{KN/\pi\Sigma}\ T_{\pi\Sigma,\bar{K}N}(I=0) \right|^2 p_{\pi\Sigma}$$

Experimental data

new data on the $\pi\Sigma$ mass spectra in various reactions !!!

HADES Collaboration (2013) - $pp \longrightarrow pK^+\pi\Sigma$
CLAS Collaboration (2013) - $\gamma p \longrightarrow K^+\pi\Sigma$
J-PARC E31 Collaboration (2016) - $K^-d \longrightarrow n\pi\Sigma$
weak decays of heavy hadrons, e.g. $\Lambda_c \longrightarrow \pi^+ MB$, $MB = \pi\Sigma$ or $\bar{K}N$

in principle, theory can accomodate the CLAS data, though dynamics of the particular process should be accounted for properly to draw any conclusion

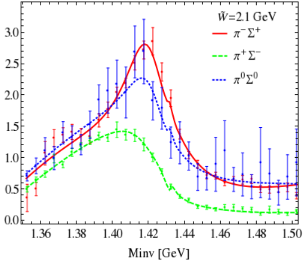

M. Mai, U.-G. Meißner - Eur. Phys. J. A 51 (2015) 30

Chirally motivated $\bar{K}N$ approaches

we discuss the available theoretical approaches based on meson-baryon chiral Lagrangian that:

- include terms up to the NLO $\mathcal{O}(q^2)$ chiral order
- fit the SIDDHARTA kaonic hydrogen $1s$ level characteristics

Schematic picture:

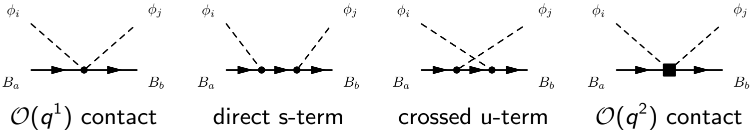

Parameters: f_π, f_K, f_η - meson decay constants

$D \simeq 3/4$, $F \simeq 1/2$ - axial vector couplings, $g_A = F + D$

b_0, b_D, b_F, four d's - second order couplings

M_0 - baryon octet mass

Some NLO LECs and M_0 fixed by GMO mass splitting formulas and by a relation to the πN sigma term,

$$\sigma_{\pi N} = -2m_\pi^2(2b_0 + b_D + b_F)$$

Chirally motivated $\bar{K}N$ approaches

- Kyoto-Munich (KM)
  Y. Ikeda, T. Hyodo, W. Weise, Nucl. Phys. A 881 (2012) 98
  - WT, LO and NLO fits
  - NLO couplings/contributions kept small
  - 15 parameters in the KM_{NLO} model
- Murcia (M)
  Z. H. Guo, J. A. Oller, Phys. Rev. C 87 (2013) 035202
  - LO and two different NLO fits
  - relatively large NLO couplings/contributions
  - 16 and 15 parameters in the M_{I} and M_{II} models, respectively
  - additional experimental data fitted, including $K^- p \longrightarrow \eta\Lambda$ to cover the $\Lambda(1670)$ region

Chirally motivated $\bar{K}N$ approaches

- Bonn (B)
  M. Mai, U.-G. Meißner - Eur. Phys. J. A 51 (2015) 30
  - comprehensive NLO fits (8 local minima found)
  - relatively large NLO couplings/contributions
  - 20 parameters in the NLO models, B_2 and B_4 seem best
  - CLAS data on $\pi\Sigma$ distributions used to sort out the χ^2 minima
  - genuine Bethe-Salpeter equation solved
- Prague (P)
  A. C., J. Smejkal, Nucl. Phys. A 881 (2012) 115
  - WT and NLO fits
  - relatively small NLO couplings/contributions
  - only 7 parameters in the P_{NLO} fit
  - separable effective potentials

$$V_{ij}(k,k';\sqrt{s}) = g_i(k^2)\, v_{ij}(\sqrt{s})\, g_j(k'^2), \quad g_j(k) = \frac{1}{1+(k/\alpha_j)^2}$$

Chirally motivated $\bar{K}N$ approaches

on-shell approaches (KM, M, B models) vs. separable potentials (P model)

both methods based on a solution of the Lippman-Schwinger equation with energy dependent potential kernel derived from a chiral Lagrangian

$$T(\sqrt{s}) = V(\sqrt{s}) + V(\sqrt{s})\, G(\sqrt{s})\, T(\sqrt{s})$$

the one-loop meson baryon integrals (Green functions) are regularized by either dimensional regularization

$$G_j(\sqrt{s}) = \frac{1}{16\pi^2}\left[a_j(\mu) + \log\frac{M_j^2}{\mu^2} + G_0(\sqrt{s}, m_j, M_j)\right]$$

$$G_0(\sqrt{s}, m_j, M_j) = -1 + \frac{m_j^2 - M_j^2 + s}{2s}\log\left(\frac{m_j^2}{M_j^2}\right) - \frac{4k_j}{\sqrt{s}}\,\mathrm{arcth}\left(\frac{2k_j\sqrt{s}}{(M_j+m_j)^2 - s}\right)$$

OR the off-shell form-factors due to separable potentials

$$G_j(\sqrt{s}) = -4\pi\int\frac{d^3p}{(2\pi)^3}\frac{g_j^2(p^2)}{k_j^2 - p^2 + i\epsilon} = \frac{(\alpha_j + ik_j)^2}{2\alpha_j}\,[g_j(k_j)]^2$$

the subtraction constants $a_j(\mu)$ and the inverse ranges α_j are related

Model predictions

kaonic hydrogen $1s$ level characteristics and $\Lambda(1405)$ poles

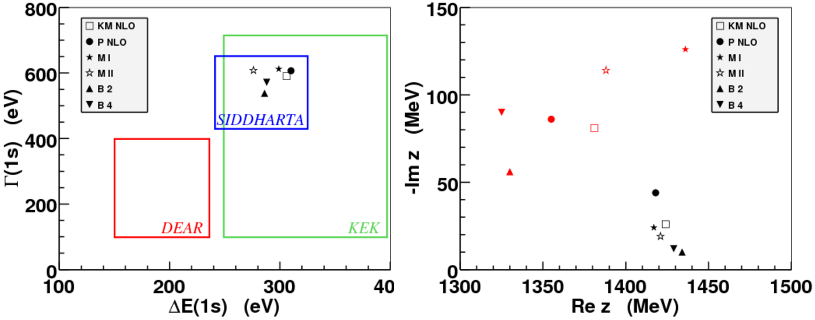

- the models are in close agreement reproducing the SIDDHARTA data
- all models tend to agree on the position of the $\bar{K}N$ related pole
- the data are not very sensitive to the position of the $\pi\Sigma$ related pole

Model predictions

$K^- p$ and $K^- n$ elastic amplitudes

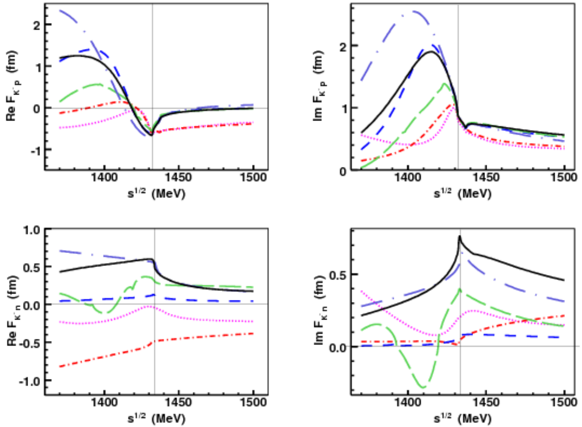

B_2 (dotted, purple), B_4 (dot-dashed, red), M_I (dashed, blue), M_{II} (long-dashed, green), P_{NLO} (dot-long-dashed, violet), KM_{NLO} (continuous, black).

Model predictions

For a comparison, uncertainty bands provided in
Y. Ikeda, T. Hyodo, W. Weise, Nucl. Phys. A 881 (2012) 98

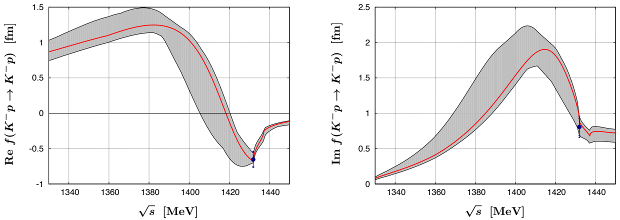

bands calculated by varying the KM_{NLO} model parameters to get the K^-p scattering length within SIDDHARTA experimental error bars

Model predictions

the theoretical ambiguities below the $\bar{K}N$ threshold are much larger than indicated by uncertainty bounds derived from variations of the $K^- p$ scattering length for a specific model and a given χ^2 local minima !!!

the $I = 1$ sector is not restricted by the fitted experimental data leading to varied predictions for the $K^- n$ scattering amplitude

New data needed !!!

- new precise data for the isovector $K^- p \longrightarrow \pi^0 \Lambda$ and isoscalar $K^- p \longrightarrow \pi^0 \Sigma^0$ reactions at as low energies as possible are highly desired
- $\pi\Sigma$ mass spectra at subthreshold energies should help provided we understand the process dynamics
- kaonic deuterium measurement (AMADEUS, Frascati) will also add to the picture

Dynamically generated resonances/poles

Where do the poles come from? (demonstration for the Prague approach)
The amplitude has poles for complex energies z (equal to $\sqrt{s}$ on the real axis) if a determinant of the inverse matrix is equal to zero,

$$\det|f^{-1}(z)| = \det|v^{-1}(z) - G(z)| = 0$$

The origin of the poles can be traced to the

zero coupling limit: $C_{ij} = 0$ for $i \neq j$ (interchannel couplings switched off)

for $C_{i,j\neq i} = 0$ the condition for a pole of the amplitude becomes

$$\prod_n [1/v_{nn}(z) - G_n(z)] = 0$$

There will be a pole in channel n at a Riemann sheet $[+/-]$ (phys./unphys.) if the following condition is satisfied for any complex energy z:

$$\frac{4\pi f_n^2}{C_{nn}(z)} \, \frac{z}{M_n} + \frac{(\alpha_n + \mathrm{i}k_n)^2}{2\alpha_n} \, [g_n(k_n)]^2 = 0$$

Only states with nonzero diagonal couplings $C_{i,j=i}$ can generate the poles!

Dynamically generated resonances/poles

What channels have nonzero diagonal couplings?
For simplicity, we first look only at the leading order WT term couplings

Sample results for the P_{WT} model:

sector	channel	ZCL state	resonance
	$\pi\Sigma$	resonance	$\Lambda(1405)$
$I = 0$	$\bar{K}N$	bound	$\Lambda(1405)$
	$K\Xi$	bound	$\Lambda(1670)$
	$\pi\Sigma$	resonance	—
$I = 1$	$\bar{K}N$	virtual	$K^- n$ amplitude
			$\pi\Sigma$ photoproduction (CLAS data)
	$K\Xi$	virtual	$\Sigma(1750)$

In general, the exact situation (existence of a ZCL pole in a given channel) depends on the model parameters (subtraction constants, NLO contributions that generate sufficiently large couplings C_{nn})

Dynamically generated resonances/poles

ZCL pole equation for the on-shell Kyoto-Munich and Murcia approaches:

$$\frac{1}{V_{nn}(z)} + \frac{1}{(4\pi)^2}\left[a_n(\mu) + 2\log\frac{M_n}{\mu} + G_0(z,m,M)\right] = 0$$

Solutions can be found as crossings of the $1/V$ plot and the meson-baryon loop function G. Example: KM_{WT} model, $K\Xi$ channel, unphysical RS

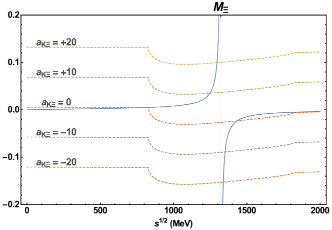

Conclusion: $a_j < a_j(\max)$ to generate a ZCL pole

Similarly, it can be shown for the Prague model $\alpha_j > \alpha_j(\min) = \frac{16\pi}{\tilde{C}_{ii}}\,\frac{f_i^2}{\omega_i}$

Dynamically generated resonances/poles

Pole movements upon scaling the nondiagonal interchannel couplings

$C_{i,j\neq i}$ replaced by $x \cdot C_{i,j\neq i}$

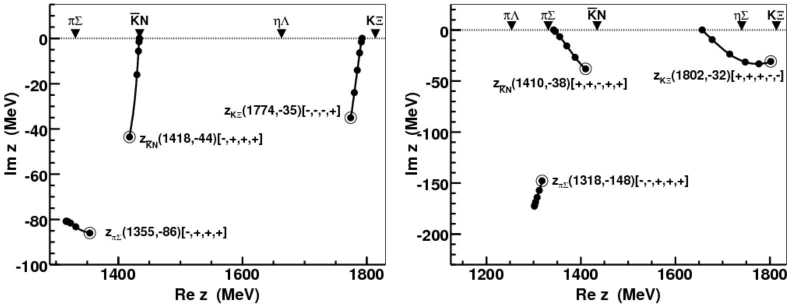

P_{NLO} model, left panel: isoscalar states, right panel: isovector states
The pole positions in the physical limit are emphasized with large empty circles.
The triangles at the top of the real axis indicate the channel thresholds.

Dynamically generated resonances/poles

Pole movements upon scaling the nondiagonal interchannel couplings

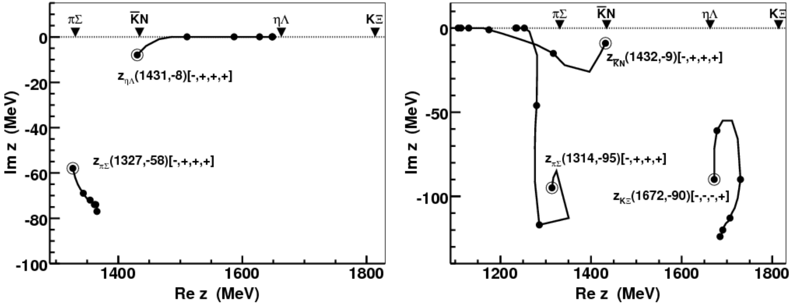

B_2 (left panel) and B_4 (right panel) models:
Only the isoscalar ($I = 0$) poles are shown with the pole positions in the physical limit emphasized by large empty circles. The triangles at the top of the real axis indicate the channel thresholds.

Dynamically generated resonances/poles

Our findings

resonance	models / ZCL channels					
	P_{NLO}	KM_{NLO}	M_I	M_{II}	B_2	B_4
$\Lambda_1(1405)$	$\pi\Sigma$	$\pi\Sigma$	$\pi\Sigma$	$\pi\Sigma$	$\pi\Sigma$	$\pi\Sigma$
$\Lambda_2(1405)$	$\bar{K}N$	$\bar{K}N$	$\bar{K}N$	$\eta\Lambda$	$\eta\Lambda$	$\bar{K}N$
$\Lambda(1670)$	$K\Xi$	—	$K\Xi$	$K\Xi$	—	$K\Xi$
$\bar{K}N(I=1)$	$\bar{K}N$	$\eta\Sigma$	$\bar{K}N$	$\bar{K}N$	—	—
$\Sigma(1750)$	$K\Xi$	—	—	$K\Xi$	—	$K\Xi$

M_{II} and B_2 models generate the $\Lambda_2(1405)$ pole from the $\eta\Lambda$ ZCL bound state.

earlier reports on the isovector $\bar{K}N$ related pole:

J. Oller, U.-G. Meißner - Phys. Lett. B 500 (2001) 263

D. Jido, J.A. Oller, E. Oset, A. Ramos, U.-G. Meißner - NPA 725 (2003) 181

A.C., E. Friedman, A. Gal, D. Gazda, J. Mareš - PRC84 (2011) 045206

A.C., J. Smejkal - Few Body Syst. 54 (2013) 1183

Summary

- Chirally motivated coupled channels models give realistic description of the $\bar{K}N$-$\pi\Sigma$ dynamics at energies close to threshold.
- The theoretical predictions for energies below the $\bar{K}N$ threshold and in the $I = 1$ sector are not restricted by the experimental data and vary significantly for the considered approaches.
- The origin of the poles of the scattering matrix can be related to poles generated in the ZCL revealing different concepts for the generation of the physically observed resonances.
- Two poles of the $\Lambda(1405)$ generated dynamically. The models can (in principle) account for the $\Lambda(1670)$ and the $\Sigma(1750)$ resonances as well.
- Some models predict the existence of an isovector state close to the $\bar{K}N$ threshold.

Thanks to my collaborators !!!

M. Mai (Bonn), U.-G. Meißner (Bonn), J. Smejkal (Prague)